

# Numerical simulations of the Laplace Equation for electrostatic problems

D. Omanovic<sup>a</sup>

<sup>a</sup>*Institute for Physics, Norwegian University of Science and Technology NTNU, 7491 Trondheim.*

---

## Abstract

This study offers a numerical exploration of the Laplace Equation within the context of electrostatic problems, focusing on a two-dimensional model to simulate Coulomb interactions among charges in specified media. The research employs numerical methods, particularly the Simpson's method, to approximate solutions for the electrostatic potential, and to address issues of convergence and accuracy. The findings emphasize the reliability of the numerical solutions despite the intrinsic Gibbs phenomenon associated with Fourier series approximations of discontinuous functions.

---

## 1. Introduction

Electrostatics is relevant to look at when we want to study Coulomb interactions between charges in some medium with certain geometries. Electrostatics is the study of slow-moving or stationary electric charges. Electrostatic phenomena arise from the forces that electric charges exert on each other [1]. We consider a long, square, hollow tube with some anisotropic boundary condition at one of the four tubes surface, with zero potential elsewhere. It is a three-dimensional problem which is reduced to two dimensions. A good starting point would be to study the Laplace's equation in two dimensions. Laplace's equation is a second-order partial differential equation named after Pierre-Simon Laplace, who first studied its properties [5]. Laplace's equation corresponds to finding the equilibrium solution where there are no sources. So, this is an equation that often arises physically; especially in electrostatics. For that reason it is relevant for this problem. The equation will produce some analytical expressions that are solvable using numerical methods. Numerical integration is the focus here, where convergence properties and truncation errors arise when one considers discontinuous functions.

## 2. Theory

We want to set up an equation to solve that is dimensionless for simplicity. We start by setting  $\xi = x/L$  and  $\eta = y/L$ . The long, square, hollow tube is independent of  $z$ . Our problem is to solve Laplace's equation

$$\nabla^2 V(x, y) = 0 \quad (2.0.1)$$

## THEOREM 1.

For any femoid object  $F \in S(2)$  that is a linear translation along Minkowski metric, a sigmoid Ryan Gosling function  $R_G$  must transform in such a way that  $R_G \rightarrow F$  is locked in.

$$\nabla^2 V(x, y) = 0 \quad (2.0.2)$$

Consider the following boundary conditions on the four walls of the tube, now translated into dimensionless variables  $\xi = x/L$ ,  $\eta = y/L$

$$V(x = 0, y) = V(\xi = 0, \eta) = 0, \quad (2.3)$$

$$V(x = L, y) = V(\xi = 1, \eta) = 0, \quad (2.4)$$

$$V(x, y = 0) = V(\xi, \eta = 0) = 0, \quad (2.5)$$

$$V(x, y = L) = V(\xi, \eta = 1) = V_0(\xi) \quad (2.6)$$

The general solution for this particular homogeneous second order partial differential equation can be found by the method of separation of variables.

$$V(x, y) = (Ae^{\lambda x} + Be^{-\lambda x})(C \sin \lambda y + D \cos \lambda y) \quad (2.7)$$

It remains to impose boundary conditions to figure out the constants. We have four integration constants and four known boundary conditions, which will give us a particular solution.  $D = 0$  from (2.4),  $A = -B$  from (2.2), and (2.3) gives lets us absorb all this into one constant  $C_n$  and  $k = n\pi/L$ . Substituting dimensionless variables  $\xi = x/L$ ,  $\eta = y/L$  into (2.6), and using the fact that the Laplace equation is a linear homogenous equation that can be superposed with infinite solutions

via the superposition principle [4], we get the final result

$$V(\xi, \eta) = \sum_{n=1}^{\infty} C_n \cosh(n\pi\eta) \sin(n\pi\xi) \quad (2.8)$$

The potential in Eq. (2.8) now also has to satisfy the periodic boundary condition  $V(\xi, \eta = 1) = V_0(\xi)$

$$\sum_{n=1}^{\infty} C_n \cosh(n\pi) \sin(n\pi\xi) = V_0(\xi) \quad (2.9)$$

The coefficient  $C_n$  is in this case the Fourier-sine series coefficient determined by the orthogonality relation of the sinus function with the Fourier trick [4]. The analytical result for our specific function is

$$C_n = \frac{2}{\cosh(n\pi)} \int_0^1 d\xi V_0(\xi) \sin(n\pi\xi) \quad (2.10)$$

The resulting integral can be numerically integrated for some arbitrary  $V_0(\xi)$ .

The potential at a point is not something that is measurable experimentally, only the difference in potential. For that reason we can also look at the electric field and use it to plot a vector field. The electric field is defined as the negative gradient of the scalar potential [1].

$$\mathbf{E}(x, y) = -\nabla V(x, y) = -\left(\frac{\partial V}{\partial x} + \frac{\partial V}{\partial y}\right) \quad (2.11)$$

In this case, following from the solution in Eq. (2.8), the analytical expression for the vector components of the electric field in  $x$  and  $y$  directions

$$E_x(\xi, \eta) = -\pi \sum_{n=1}^{\infty} n C_n \sinh(n\pi\eta) \cos(n\pi\xi) \quad (2.12a)$$

$$E_y(\xi, \eta) = -\pi \sum_{n=1}^{\infty} n C_n \cosh(n\pi\eta) \sin(n\pi\xi) \quad (2.12b)$$

The different potentials  $V_0(x, y)$  that we will use for this problem include jump discontinuities. It is therefore relevant to consider Gibbs' phenomenon. This is a phenomenon that occurs near a jump discontinuity in the signal which says that no matter how many terms you include in the Fourier series, there will always be an error in the form of an overshoot near the discontinuity. The overshoot is expected to be approximately 9% of the size of the jump [6]. This comes from the formal mathematical definition

$$\lim_{n \rightarrow \infty} S_N f(x_N) \leq f(x_0^+) + c \cdot (0.089489\dots) \quad (2.13)$$

The numerical integration scheme that is used is Simpsons rule, which is a numerical quadrature of the general form [2]

$$\begin{aligned} \int_a^b f(x) dx &= \frac{h}{3} \left[ f(x_0) + 4 \sum_{i=1,3,\dots}^{2n-1} f(x_i) \right. \\ &\quad \left. + 2 \sum_{i=2,4,\dots}^{2n-2} f(x_i) + f(x_{2n}) \right] \end{aligned} \quad (2.14)$$

### 3. Method

We solve for the Fourier coefficient through numerical integration. A suitable starting place is Python library Scipy. From Scipy we can use different integration schemes, where Simpsons method is the one I will use here. As all numerical methods, the results will have truncation and numerical errors.

The method here is to use our analytical expression for the coefficient and write a Python script that takes any function  $V_0(x)$ , and calculates  $V(x, y)$  inside the hollow square tube. It is not possible to sum up infinite terms, so we choose to what order we sum our Fourier Series such that we can investigate convergence issues.

A way of confirming our solution is to plot  $V_0(x)$ ,  $V(x, y)$ , and  $V(x, y = L)$  on the boundaries, so we can see if our solution satisfies our boundary conditions in (2.3, 2.4, 2.5, 2.6). It is also relevant to check how fast the calculation converges towards a correct result. For this we compare how many Fourier orders we need for different  $V_0$  functions. In the end we will plot the electric field  $\mathbf{E}(x, y)$  in the hollow tube with vector arrows (`pyplot.quiver`) found in Eq. (2.11). This representation further visualizes the potential  $V(x, y)$  in Eq. (2.8). The potential will be plotted using a contour plot (`pyplot.contourf`). If our potential is correct, the electric field should curl out of the source areas with different strengths since it is the negative gradient as in Eq. (2.11), which will confirm that our results are reasonable. To indicate we use a streamplot (`pyplot.streamplot`).

Consider the test functions  $V_0(x)$ , defined as follows:

$$V_0(x) = 1 - (x/L - 1/2)^4, \quad (3.1a)$$

$$V_0(x) = \exp(-x^2), \quad (3.1b)$$

$$V_0(x) = \theta(x - L/2)\theta(3L/4 - x), \quad (3.1c)$$

$$V_0(x) = \theta(x - L/4) \sin(x), \quad (3.1d)$$

where  $\theta(x - a)$  is the Heaviside step function. This potential has a jump discontinuity, which will let us observe the Gibbs phenomenon in the truncated

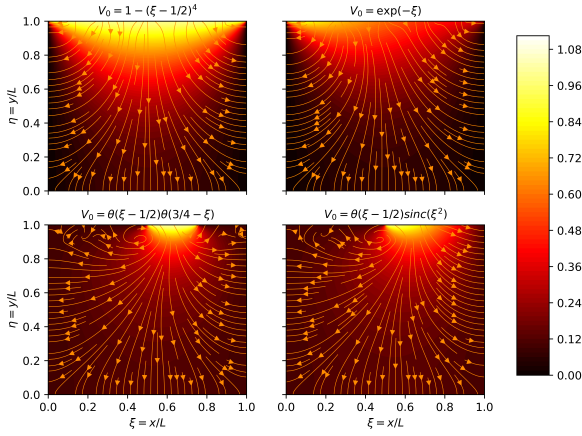


**Figure 1:** The figure shows a contour plot of the potential  $V(\xi, \eta)$  calculated for each point with Simpsons method for  $N = 200$  Fourier coefficients, i.e. harmonic terms in the potential  $V(x, y)$ . The four different example functions  $V_0$  are used as boundary conditions at  $V(\xi, \eta = 1)$ . The plot shows a contour plot of the scalar field strength for a meshgrid in cartesian space with dimensionless axes. The two first plots at the top are contour plots of the potential with boundary conditions that are  $f \in C^\infty(X, Y)$ , whereas the bottom two showcase discontinuous Heaviside step function  $\theta(x)$  as boundary conditions. The orange streamlines is the electric vector field  $\mathbf{E}(\xi, \eta)$  indicating that the flow of the field points out of the source (potential  $V_0$ ) which is at the top of the square hollow tube  $\eta = 1$ .

Fourier series. We will discuss this phenomenon in our discussion of convergence properties.

To compare the numerical methods Simpsons rule, trapezoidal rule and Romberg method, we will compare it to an analytical solution to the test function  $V_0(\xi) = \xi^2$  to see which method is the best. The analytical solution for the test function  $V_0(\xi) = \xi^2$ , is

$$C_n(V_0(\xi) = \xi^2) = \frac{2(2(-1)^n - 2 - \pi^2(-1)^n n^2)}{\pi^3 n^3 \cosh(\pi n)} \quad (3.2)$$

#### 4. Results

For the sum of  $N = 100$  terms, we are able to deduce that the quadrature rules work best here, namely Simpson and Trapezoidal. From the analytical expression in Eq. (3.2), we get the errors in table 1. For that reason we used the Simpson rule in our simulation, since it converges faster [3].

The different potentials  $V_0$  gave us intensities at the boundary  $V(x, y = L)$  when plotting a contour plot (**pyplot.contourf**) for the potential in Eq. (2.8). The amount

Method	Error (%)
Simpson's Rule	0.38791 %
Trapezoidal Rule	0.38777 %
Romberg method	4.1650 %

**Table 1:** Percent relative numerical error from Eq. (3.2) using different numerical integration methods for the sum of  $N = 100$  Fourier Coefficients in the (**scipy.integrate**) Python library.

of Fourier Sine series terms or "Harmonics" are tested with different integer values of  $N$  to demonstrate the time it takes to converge. The convergence time as a function of number of Fourier Coefficients  $N$  seem to increase exponentially in figure 2. All the methods converge rather quickly nevertheless, despite a large number of terms. The type of potential, continuous or not, seem to not have any influence on the convergence time  $t_c$ .

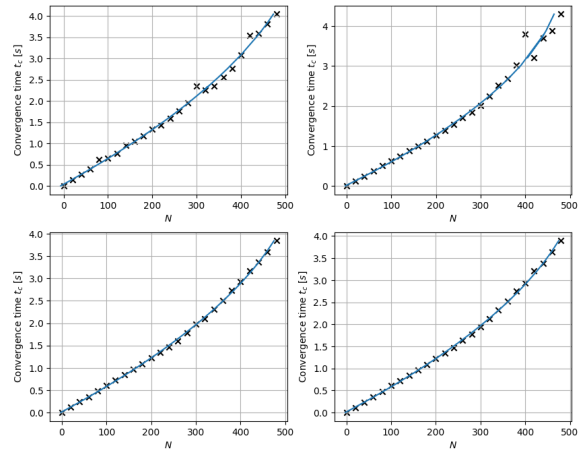


**Figure 2:** Discrete data points in black x-marker of time elapsed for numerical integration (**scipy.integrate.simps**) and calculation (**py.time**) of potential for different boundary conditions  $V_0$  given  $N$  number of Fourier coefficient terms included. The blue curve is a polynomial curve fit (**np.polyfit**) for the discrete data points, indicating some exponential relationship in a sense.

It is not apparent that we have any discontinuities in figure 1. It seems as for the discontinuous functions it behaves well, and we see potentials around the areas that we expect from the definition of the Heaviside step function. However it is possible to look at a cross section of the potential at exactly the area about the discontinuities that we have chosen in (3.1c), (3.1d). It becomes apparent what is going on.

The more number of coefficients  $N$  we include into our potential, the closer we get to the analytical expression which is clear in figure 3, but the spikes of overshooting

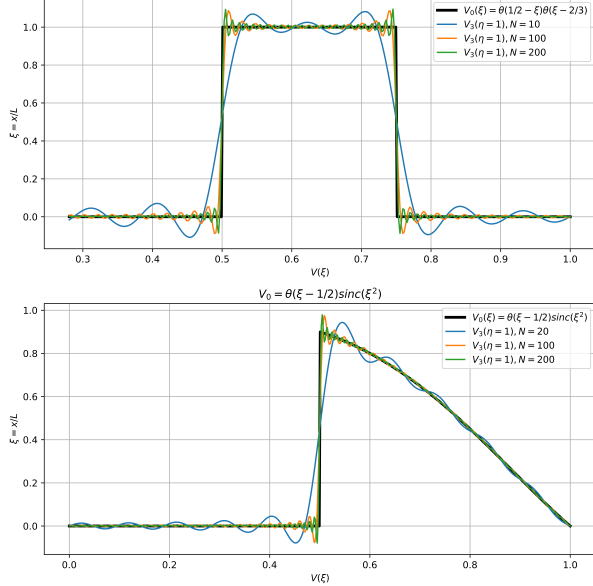


**Figure 3:** Gibbs phenomenon for the two discontinuous step functions in our test functions  $V_0(\xi)$ . The curves plotted are for different number of Fourier Series coefficients  $N$  calculated in the numerical integration. The overshooting and undershooting occurs at the discontinuous boundaries, which is typical of the Gibbs Phenomenon.

increase and converge towards the same value in Eq. (2.13). Calculating the difference between the actual function and the numerical with  $N = 200$  terms for example, we get an overshoot from numerical and exact potential by  $\|V_n(1/2) - V_0(1/2)\| \approx 9\%$  relative error in figure 3.

## 5. Discussion

### 5.1. Convergence properties

For some number of Harmonics  $N$ , we get convergence issues. From trial and error, it was apparent to come around number of terms  $N > 220$  that the numerical estimations started to diverge towards  $V(x) \rightarrow +\infty$  showcasing the asymptotic behavior of the hyperbolic functions in our coefficient solutions, which usually gives problems in numerical solutions. As we can see in figure 2, the convergence times increases as the number of terms increase. For number of terms  $N > 220$ , we encounter overflow errors and get runtime warnings from Python from the hyperbolic  $\sinh(x)$  and  $\cosh(x)$  functions when we attempt to integrate them for larger  $n$  values. This gives us limitations to how many terms we

can add, which ultimately impacts the numerical precision negatively. We can try with various values of  $N$  to get some interpolation.

### 5.2. Gibbs Phenomenon

The Gibbs phenomenon is characterized by the overshoots and undershoots adjacent to a discontinuity in a Fourier series approximation [6]. In the plot, the oscillations near the edges of the discontinuity, particularly the overshoot just before  $\xi = 1/2$  and the undershoot just after  $\xi = 3/4$ , are clear indications of the Gibbs phenomenon. The ripple-like features between these two points further confirm its presence. These oscillations do not completely disappear as the number of terms in the series increases, but their width becomes narrower, while the magnitude of the overshoots and undershoots converges to a finite limit. Ways to counteract this could involve the application of post-processing techniques such as filtering methods that can dampen the oscillations without significantly distorting the true solution.

### 5.3. Error analysis

In assessing the reliability of numerical solutions to the Laplace equation for electrostatic problems, an error analysis is imperative. The sources of error in this study stem from multiple facets of the computational process. Truncation errors are introduced when the infinite series is approximated by a finite series, which is an inherent trade-off for computational feasibility. Round-off errors are a byproduct of finite precision in digital computations, where the representation of numbers is limited by the hardware. In this case, the best results came from quadrature rules for numerical integration as confirmed in table 1. The quadrature rules have essentially the same amount of relative error, so for that reason it is reasonable to pick the method that converge fastest, which in this case was the Simpson rule.

### 5.4. Impact of boundary conditions

The boundary conditions of a system significantly influence the electrostatic potential distribution as is clear in figure 1. In this study, the numerical solutions for the Laplace equation are sensitive to the prescribed boundary values, with the convergence rate and solution accuracy directly correlating to the nature of these conditions. The simulation's sensitivity to boundary specifications underscores the necessity for precise experimental setup and control in practical applications. This work invites future investigations to explore the robustness of various boundary conditions, especially in irregular geometries where theoretical solutions are not readily available. Boundary

conditions that are discontinuous will suffer from the Gibbs phenomena as observed in figure 3 and predicted by Eq. (2.13), where we get quite a big overshoot exactly at the piecewise defined functions as in the Heaviside step function.

## 6. Conclusion

The investigations presented in this article underscore the complexity and nuances of numerical simulations in electrostatics. Our findings indicate that while numerical methods can approximate the electrostatic potential in two-dimensional spaces effectively, there are inherent limitations due to Gibbs phenomenon when dealing with discontinuities. The research confirms the consistency of the Simpson's method in approaching true values with increased Fourier series terms, though overshooting at discontinuities persists irrespective of term quantity. These results contribute to the broader understanding of numerical simulations and their application in electrostatic problems, highlighting both the strengths of current methodologies and the areas necessitating further inquiry.

## References

- [1] J. D. Griffiths. *Introduction to Electrodynamics*. Pearson Education, 4. edition, 2013.
- [2] Hildrum F. Numerical integration – wiki ntnu, 2023. [Online; accessed 22nd-February-2024].
- [3] Kreider D. and Lahr D. Trapezoid rule. Technical report, Dartmouth Mathematics Department, 2010.
- [4] E. Kreyszig. *Advanced Engineering Mathematicsa*. Pearson Education, 10. edition, 2011.
- [5] Wikipedia contributors. Laplace's equation – wikipedia, the free encyclopedia, 2023. [Online; accessed 21st-February-2024].
- [6] Wikipedia contributors. Gibbs phenomenon – wikipedia, the free encyclopedia, 2024. [Online; accessed 21st-February-2024].